Geo-Mar Lett (2011) 31:51–64
DOI 10.1007/s00367-010-0213-z

ORIGINAL

Erosion of continental margins in the Western Mediterranean due to sea-level stagnancy during the Messinian Salinity Crisis

Janna Just · Christian Hübscher · Christian Betzler · Thomas Lüdmann · Klaus Reicherter

Received: 13 October 2009 / Accepted: 23 June 2010 / Published online: 15 July 2010

Abstract High-resolution multi-channel seismic data from continental slopes with minor sediment input off southwest Mallorca Island, the Bay of Oran (Algeria) and the Alboran Ridge reveal evidence that the Messinian erosional surface is terraced at an almost constant depth interval between 320 and 380 m below present-day sea level. It is proposed that these several hundred- to 2,000-m-wide terraces were eroded contemporaneously and essentially at the same depth. Present-day differences in these depths result from subsidence or uplift in the individual realms. The terraces are thought to have evolved during one or multiple periods of sea-level stagnancy in the Western Mediterranean Basin. According to several published scenarios, a single or multiple periods of relative sea-level stillstand occurred during the Messinian desiccation event, generally known as the Messinian Salinity Crisis. Some authors suggest that the stagnancy started during the refilling phase of the Mediterranean basins. When the rising sea level reached the height of the Sicily Sill, the water spilled over this swell into the eastern basin. The stagnancy persisted until sea level in the eastern basin caught up with the western Mediterranean water level. Other authors assigned periods of sea-level stagnancy to drawdown phases, when inflowing waters from the Atlantic kept the western sea level constant at the depth of the Sicily Sill. Our findings corroborate all those Messinian sea-level reconstructions, forwarding that a single or multiple sea-level stagnancies at the depth of the Sicily Sill lasted long enough to significantly erode the upper slope. Our data also have implications for the ongoing debate of the palaeo-depth of the Sicily Sill. Since the Mallorcan plateau experienced the least vertical movement, the observed terrace depth of 380 m there is inferred to be close to the Messinian depth of this swell.

J. Just (✉) · C. Hübscher
Institute of Geophysics, University of Hamburg,
20146 Hamburg, Germany
e-mail: janna.just@uni-bremen.de

C. Betzler
Institute for Geology and Paleontology, University of Hamburg,
20146 Hamburg, Germany

T. Lüdmann
Institute of Biogeochemistry and Marine Chemistry,
University of Hamburg,
20146 Hamburg, Germany

K. Reicherter
Department of Neotectonics and Natural Hazards, RWTH,
52056 Aachen, Germany

Present Address:
J. Just
Faculty of Geosciences, University of Bremen,
Klagenfurter Strasse,
28359 Bremen, Germany

Introduction

During the Messinian, tectonic uplift caused the closure of the Mediterranean–Atlantic connection, which consisted of several gateways in southern Spain and northern Africa (Esteban et al. 1996). The Iberian corridors became restricted prior to the Messinian (Martín et al. 2001; Betzler et al. 2006). The closure of the African gateways caused a substantial sea-level drop within the entire Mediterranean basin, triggering the Messinian Salinity Crisis (MSC; Hsü et al. 1973; Ryan and Cita 1978; CIESM 2008; Ryan 2009). The resulting sub-aerial exposure caused massive erosion of the continental slopes (Rizzini et al. 1978; Clauzon et al. 1996; Lofi et al. 2005; Sage et al. 2005; Bertoni and Cartwright 2006, 2007; Maillard et al. 2006). The sea-level

fall further resulted in an increased salinity of Mediterranean water and in the precipitation of evaporites. An overview of various models regarding the timing, duration and degree of sea-level fluctuations during the MSC has recently been presented by CIESM (2008). Notably, basinal evaporites up to some km in thickness have been intensely studied by means of seismic reflection surveys, revealing differences west and east of the Sicily Strait (Fig. 1; see below). Based on individual water budgets for the basins, it has been speculated that, during the MSC, the western and eastern basins became separated at the Sicily Sill, located southwest of Sicily.

Because the Sicily Sill is located in the southern part of the Apennines-Calabrian arc (e.g. Dewey et al. 1989; Gueguen et al. 1998; Gelabert et al. 2002), a tectonically active zone, its depth cannot be precisely reconstructed with available data. Nevertheless, Blanc (2006) demonstrated that the timing of accumulation of evaporites in the western and eastern basins is directly linked to the depth position of this swell. During an early phase of the MSC, the western basin water level supposedly reached the sill's top, and the water level remained constant for some thousand years in this basin, while inflowing water from the Atlantic was bypassed from the western to the eastern basin.

Alternatively, numerical simulations of Messinian sea-level fluctuations by Meijer and Krijgsman (2005) and Gargani and Rigollet (2007) showed that, from the time of sea-level drop below the Sicily Sill, the two basins evolved individually. Later, during the reflooding stage (Zanclean flood) of the Mediterranean Sea, the western basin was filled first until the height of the sill was reached (Meijer and Krijgsman 2005). Afterwards, the water spilled over the sill into the eastern basin, where sea level started to rise. The assumption underlying the model of Meijer and Krijgsman (2005) was that the inflow rate of Atlantic water into the Mediterranean Sea equalled that of the present day. This means that the geometry of the Gibraltar Strait would have been the same as today. Furthermore, the depth of the Sicily Sill was assumed to have been 300 m relative to global sea level (i.e. equal to its present-day depth). However, neither the inflow nor the depth of the sill are precisely known. Accepting the assumptions of Meijer and

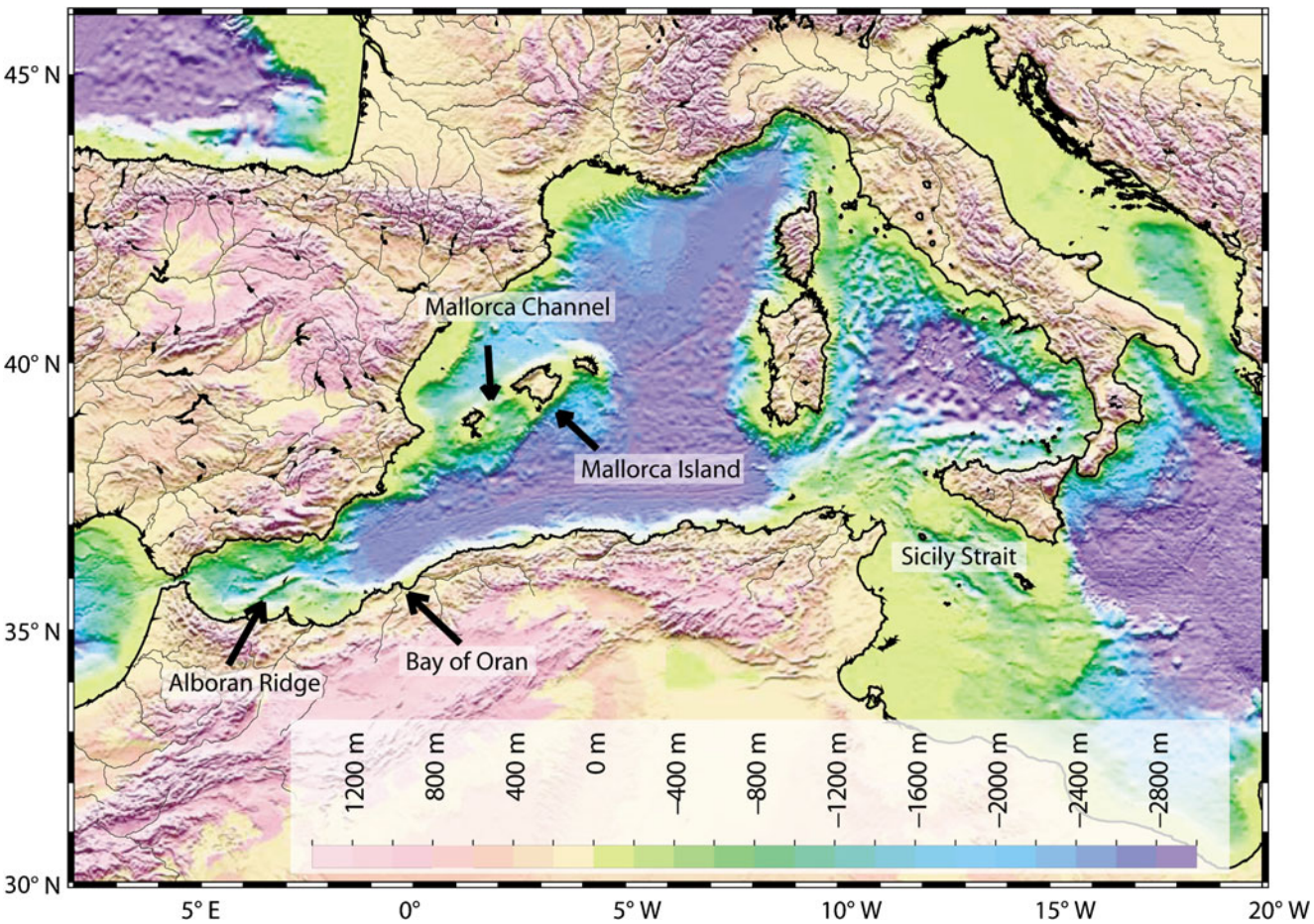

Fig. 1 Bathymetric map of the Western Mediterranean basin, with the study areas indicated by *arrows* (GEBCO One Minute Grid). The western and eastern basins are separated by the Strait of Sicily

Krijgsman (2005), the bypass period of western Mediterranean waters flowing into the eastern basin would have lasted for some thousands of years, until sea level in the eastern basin reached the height of the Sicily Sill. During this time interval, sea level in the western basin would have remained constant (Meijer and Krijgsman 2005; Fig. 2). However, by examining the scenario for a wider and deeper Gibraltar Strait geometry, and the resulting higher inflow rate, Meijer and Krijgsman state that the refilling of the Mediterranean could have been completed much faster. According to Gargani and Rigollet (2007), repeated sea-level fluctuations occurred during the MSC. It can be hypothesized that recurring sea-level stagnancy at the height of the Sicily Sill accompanied each refilling phase.

Blanc (2002) modelled the Zanclean flood in terms of erosional mechanisms at the gateway between the Atlantic and Mediterranean, proposing that a change in geometry due to erosion resulted in increased inflow rates and flow velocities and, consequently, a much faster (11 years) refilling of the Mediterranean. Recently, Garcia-Castellanos et al. (2009) observed erosive channels in the subsurface west and east of the Gibraltar Strait, based on seismic and well data. They concluded that these channels are interconnected and that they were eroded during the terminal flooding of the Mediterranean, and calculated dramatically high inflow rates and velocities at the Gibraltar Strait. The refilling of the western basin would have occurred within 500 days until the height of the Sicily Sill was reached, followed by a 300-day overspill phase into the eastern basin and another 150 days until complete refilling of the entire Mediterranean.

Sea-level stillstands are inherent to both conflicting models described above. In the case of an extended stagnancy in the western Mediterranean basin, however, erosional cliffs and terraces are expected to have formed at the corresponding position of sea level. Although numerous studies based on seismic reflection data indicate sub-aerial erosion during the MSC, there is a lack of systematic investigations of the Messinian Unconformity at shallow depths. More precisely, for the identification of any erosional features linked to sea-level stagnancies at the level of the Sicily Sill, extensive mapping of this depth interval is needed. Indeed, interpretation based on single profiles is problematic for the discrimination between erosional terraces and other features like incised valleys, fault scarps or head scarps of submarine slides.

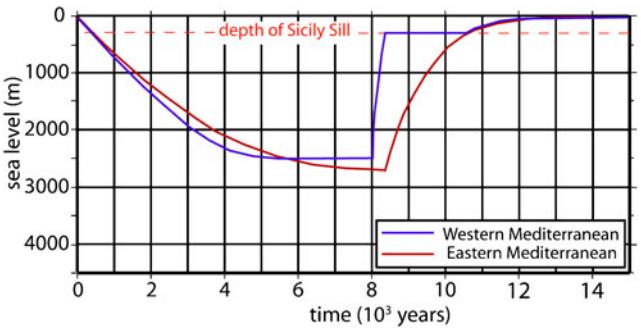

Fig. 2 Modelled sea-level curves for the Western and Eastern Mediterranean (from Meijer and Krijgsman 2005). The sea level in the western and eastern basins evolved differently from the time it dropped below the depth of the Sicilian Sill. The assumptions for this model are the present-day geometry and inflow rates at the Gibraltar Strait and a depth of the Sicily Sill of 300 m. The reflooding of the western basin was rapid until sea level reached the height of the sill, after which sea level remained constant for about 2,000 years

In search of evidence of such sea-level stagnancies at the Sicily Sill, and of the duration of stagnant water levels in the Western Mediterranean, we evaluated seismic reflection data from the south-western shelf of Mallorca Island, the Bay of Oran and the Alboran Ridge (Fig. 1), collected in summer 2006 during the CARBMED research cruise M69/1 aboard the R/V *Meteor* (Hübscher et al. 2010). The data further allow constraining the palaeo-depth of the Sicily Sill.

Messinian Salinity Crisis

Deep basin stratigraphy

Current understanding of the Messinian palaeo-environment is based mostly on studies of exposed sedimentary successions in peri-Mediterranean basins (e.g. Crete, Sicily, Cyprus, southern Spain; Clauzon et al. 1996; Riding et al. 1998; Butler et al. 1999; Rouchy and Caruso 2006). However, such marginal basins represent only ~5% of all Messinian evaporites. Our knowledge of the deep basinal evaporites comes largely from seismic reflection data, which can be considered as the most important archive of Messinian environmental changes (Hübscher et al. 2007). Seismic units of MSC deposits have been investigated in several sub-basins of the Western Mediterranean, including along the Ligurian margin (Savoye and Piper 1991), and in the Gulf of Lion (Lofi et al. 2005) and the Valencian Basin (Maillard et al. 2006). Here, three units with distinct seismic facies have been identified (Montadert et al. 1970), formerly labelled the lower evaporite, salt and upper evaporite units. Recently, the nomenclature has been modified to the lower, mobile and upper units respectively (Lofi et al. 2010). East of the Sicily Strait, seismic studies of basinal evaporites concentrated on the Cyprus Arc (Bridge et al. 2005; Hall et al. 2005; Hübscher et al. 2009), the Nile cone (Loncke et al. 2004, 2006) and the Levantine Basin (Mart and Bengai 1982; Garfunkel and Almagor 1984; Cohen 1993; Bertoni and Cartwright 2006, 2007). Up to six evaporitic sequences can be traced throughout the Levantine Basin (Hübscher et al. 2007). The differing stratigraphy of basinal evaporites west

and east of the Sicily Sill suggests a separation of the Western and Eastern Mediterranean basins and, consequently, individual water budgets being responsible for the formation of evaporitic sequences.

Messinian erosional surfaces

The MSC sea-level drawdown resulted in sub-aerial exposure of the continental slopes and triggered massive erosion, canyon development, and the deposition of detritus on the lower slopes and adjacent fringing abyssal plains (Rizzini et al. 1978; Clauzon et al. 1996; Lofi et al. 2005; Sage et al. 2005; Bertoni and Cartwright 2006, 2007; Maillard et al. 2006, 2010). Several erosion surfaces have been evidenced on seismic data, labelled as the MES (for margin erosion surface, after Sage et al. 2005), BES (for bottom erosion surface, after Maillard et al. 2006), IES (intermediate erosion surface) and TES (for top erosion surface, after Maillard et al. 2006). For a recent detailed overview, the reader is referred to Lofi et al. (2010) and references therein.

The MES is a widespread unconformity commonly interpreted as resulting from several phases of sub-aerial erosion. It is overlain by Plio-Pleistocene deposits and extends downslope to the onlap point of the deep basin Messinian trilogy deposits. There it passes laterally to the BES, TES and IES, each of these erosion surfaces being defined based on their relationship to the downslope Messinian units. Since the pre-Messinian marine sediments were eroded mainly during the MSC, there is a sharp contrast between the reflection characteristics of the consolidated strata beneath the MES and of the lower Pliocene strata deposited under marine conditions after the reflooding of the Mediterranean (Barber 1981; Stampfli and Höcker 1989; Lofi et al. 2005).

Physical and tectonic setting

The Mediterranean Sea is a semi-enclosed marginal sea located between southern Europe and North Africa, connected to the Atlantic Ocean through the Strait of Gibraltar, and comprising a western and an eastern basin (Fig. 1), each consisting of several sub-basins. The gateway between the western and eastern basins is a relatively narrow seaway around Sicily, separating the Italian peninsula from North Africa. At the Sicily Sill, the present-day water depth is about 300 m.

The Western Mediterranean has undergone a complex tectonic evolution, Gelabert et al. (2002) recognizing three stages: during the first stage, which lasted from the latest Cretaceous until the Eocene–Oligocene transition, E-W-striking subduction of Tethyan oceanic crust beneath the Iberian and the Austroalpine–Apulian plate occurred. During the Early Oligocene (second stage), the Balearics, Corsica and Sardinia collided with Iberia and the continental blocks of the Internal Zone of the Betics and Rif (Jolivet and Faccenna 2000). From the Late Oligocene until the Middle Miocene (third stage), extensional conditions led to thinning of the continental crust in basins and the formation of back-arc basins (e.g. Gelabert et al. 2002).

The opening of the western Mediterranean basins occurred during the last 30 Ma. The westward subduction (Apennines-Maghrebides arc) of Tethyan crust initiated an extensional tectonic regime in the back-arc zone (e.g. Dewey et al. 1989; Gueguen et al. 1998; Gelabert et al. 2002). Due to changing convergence rates and velocities, the subduction zone retreated eastwards to its present-day position beneath the Italian peninsular, reaching down to Calabria and turning west via Sicily to the North African margin (for details see Gueguen et al. 1998; Faccenna et al. 2001).

Sicily Strait

The Central Mediterranean has a complex tectonic history because of the convergence between Africa and Europe (see above). Sicily is located above the Apennines-Calabrian convergence zone and was therefore affected by complex tectonics during the Cainozoic.

The tectonic configuration of the Sicily Strait has been reconstructed for Eocene to Recent times by Reeder et al. (2002). During the Eocene, Neo-Tethyan crust existed between southern Europe (Corsica, Sardinia and the Balearic Islands) and northern Africa (Tunisia, Sicily; Dewey et al. 1989). During the Oligocene and Miocene, the eastward retreat of the Apennines-Calabrian arc caused a reorganisation of the plate boundaries. By the end of the Miocene, the present-day tectonic configuration was developed (Dewey et al. 1989; Reeder et al. 2002). Using the base levels of Western Mediterranean rivers incised during sea-level stagnancy in the western basin, Blanc (2006) reconstructed the depth of the Sicily Sill during the MSC as ranging from 350–400 m relative to present-day sea level.

SW shelf of Mallorca Island

The study area off Mallorca Island comprises the SW shelf and shelf slope in prolongation of the Campos Basin (Fig. 3). The shelf is between 100 and 150 m deep, and the seafloor descends in a SW direction to the Mallorca Channel, where water depths reach 1,000 m. In the southeast the shelf is bounded by the Emile Baudot Escarpment, which has a very steep slope, descending to water depths exceeding 2,400 m.

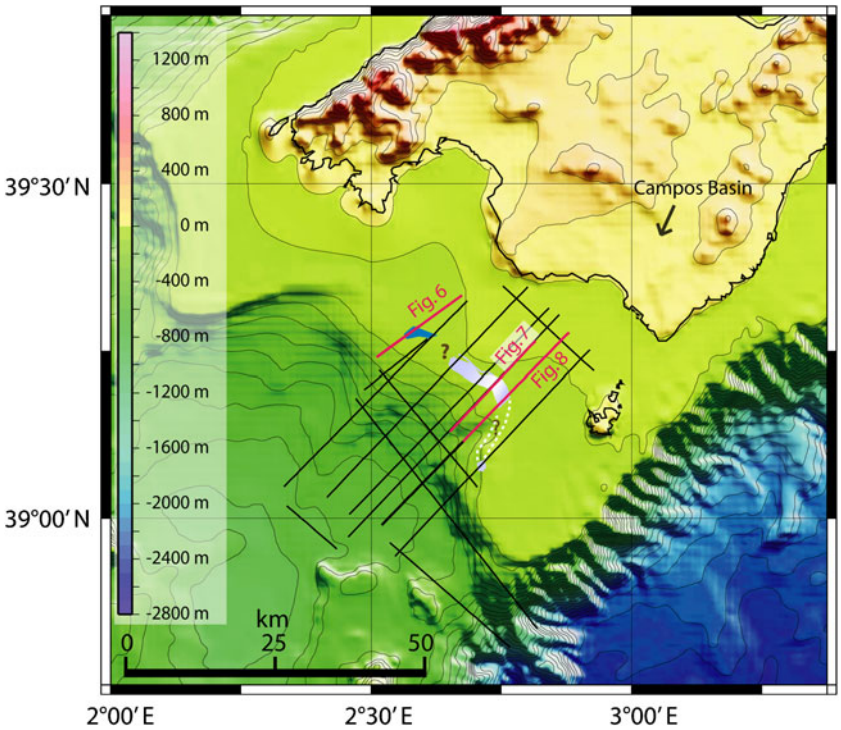

Fig. 3 Bathymetric map (m) of the SW shelf off Mallorca Island. *Lines* Seismic profiles, *red lines* profiles shown in Figs. 6, 7 and 8; *violet* mapped wide terraces with cliffs, *white* change in dip of the MES; *dotted lines* inferred continuation of terraces between the profiles

During the latest Oligocene and the Early Miocene, the anticlockwise rotation of the Corso-Sardinic block (Montigny et al. 1981) led to extension and crustal thinning between Iberia and the Balearic Promontory. As a consequence, the Valencian Trough was opened (Vegas 1992). During the Early Miocene, the Alboran Microplate started to drift westwards, thereby imposing a compressional tectonic regime on the Balearics. Mesozoic rocks, consisting mainly of carbonates (Barnolas and Simó 1984; Alvaro et al. 1989), were incorporated into the Alpine fold-and-thrust belt during this phase. In the Late Miocene, the persisting rotation of the Corso-Sardinic block and the opening of the South Balearic-Algerian Basin caused an extensional regime on Mallorca. During this phase evolved both the main horst and graben structure, consisting of Mesozoic and partially Palaeozoic basement (Jenkyns et al. 1990), and the small basins on the island (Pomar 1979). From Miocene to Pliocene times, carbonate sediments accumulated in these basins, onlapping onto the faulted blocks (Pomar and Ward 1994; Alonso-Zarza et al. 2003 and references therein).

The SW shelf of Mallorca represents the seaward prolongation of the upper Miocene Llucmajor carbonate platform and of the Campos Basin. The top of the Llucmajor platform lies today about 70 m above sea level. The Campos Basin subsided during the Pleistocene (Pomar and Ward 1994). Mesozoic and Neogene carbonates are only slightly tilted, due to normal and strike-slip faulting (Pomar 2001).

Earlier seismic data of the Mallorca Channel and the continental slope adjacent to our study area were acquired by Acosta et al. (2001, 2003, 2004), showing an unconformity truncating the poorly to well stratified underlying unit. They interpreted this horizon as the MES (labelled Messinian Unconformity in Acosta et al. 2001, 2003, 2004). In the Mallorca Channel, the MES is at a relatively deep position (approx. 1 s two-way traveltime; Acosta et al. 2004), but ascends to approx. 0.5 s TWT at the shelf slope (Acosta et al. 2001). The unconformity shows an irregular topography and has an erosional appearance. Above this horizon, two units were interpreted to have been deposited during the latest Messinian to Quaternary. According to Acosta et al., the post-Messinian succession is faulted due mainly to gravitational, rather than deep-rooted processes (cf. the latter would indicate vertical movement). One of their published survey lines extends into our new survey area, thus allowing correlating the stratigraphy in both datasets.

Bay of Oran

The Bay of Oran is semi-oval in shape and extends 30 km in a W–E direction. The study area includes the shelf and the continental slope down to a water depth of 1,000 m (Fig. 4). The Yusuf Fault is a NW-SE-oriented strike-slip fault which takes a W–E direction west of the Bay of Oran (Ballesteros et al. 2008). According to Domzig et al. (2006), a branch of this fault may extend into the region of the bay (Fig. 4).

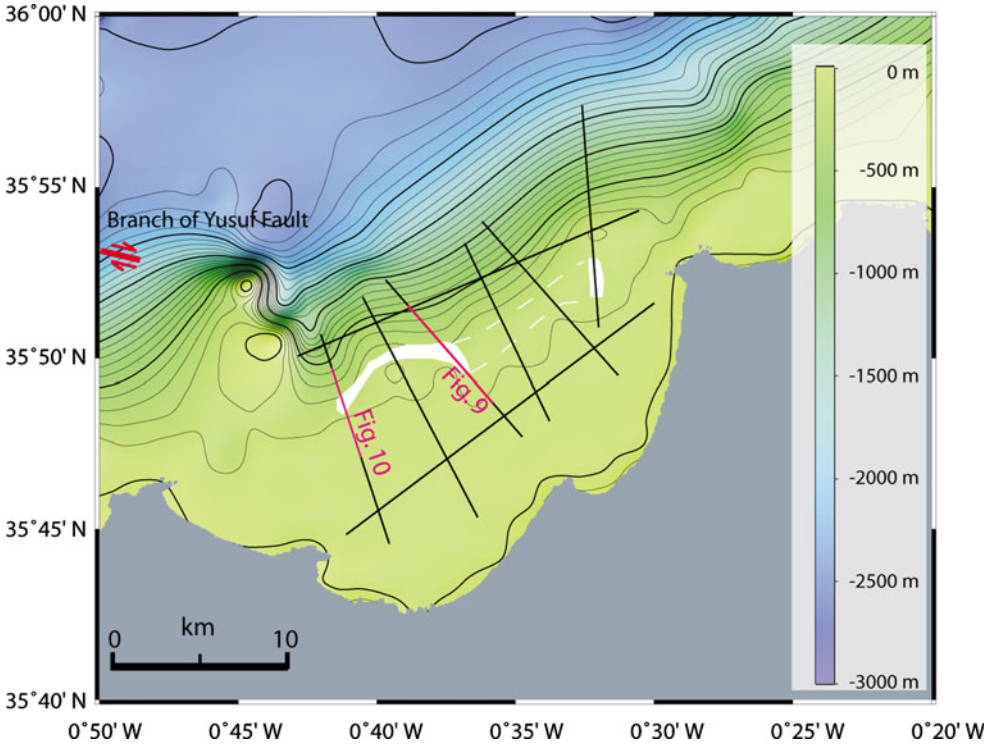

Fig. 4 Bathymetric map (m) of the Bay of Oran (Algeria). *Lines* Seismic profiles, *red lines* profiles shown in Figs. 9 and 10; *white* mapped terraces of the MES correlated between the profiles; *dotted lines* inferred continuation of terraces between the profiles

The structural and geological setting in the vicinity of Oran is dominated by the southward thrusts of the External Tell, which formed during the Alpine continental collision (de Lamotte et al. 2000). Folded and faulted Mesozoic carbonates of the former southern margin of the Tethys are unconformably overlain by post-orogenic Miocene marine to coastal sediments (Cornet et al. 1952). From adjacent areas southwest of Oran, some Messinian carbonate platforms are known which evolved on folded Mesozoic basement (Rouchy and Saint Martin 1992; Cornée et al. 1994 and references therein). The continental margin is characterized by a steep north-dipping escarpment, with possible normal faulting. Onshore, marine terraces of the last interglacial (marine isotope stage 5) have uplifted at rates of approx. 0.02 mm/year (Bouhadad 2001), indicating active deformation in Oran Bay. Betzler et al. (2010) observed that Holocene carbonate production occurs on the shelf in the bay itself. Also, those authors found siliciclastics close to the modern shoreline, but not on the outer shelf.

At present, seismic activity in the region of Oran is moderate in terms of intensity or magnitude, and characterised by long recurrence periods (Bouhadad 2001), two M<5 earthquakes having occurred in 1889 and 1959. Stronger seismic events were recorded in 1790 (Oran, intensity I=XI) and 1994 (Mascara earthquake, M 6.0), with a high death toll (Ayadi et al. 2002). Generally, the focal mechanisms showed thrust-related dissolution (Bouhadad 2001), whereby strike-slip faults had a dextral component on N110-130-trending fault planes (Ayadi et al. 2002). This is in accordance with the movement and seismicity along the Yusuf Fault in the western Alboran Sea. Existing bathymetry and seismic data for the Oran region do not show any significant recent offshore tectonic activity, with the exception of the Yusuf Fault (Domzig et al. 2006).

Alboran Ridge

The Alboran Ridge is a SW–NE elongated basement high with a length of 180 km and a width of 30 km (Fig. 5), rising up to 1,000 m above the surrounding abyssal plain and forming Alboran Island. The ridge consists of magmatic and metamorphic rocks (Maldonado et al. 1992 and references therein), while Alboran Island is composed mainly of volcaniclastic rocks on a metamorphic basement (Hoernle et al. 2003). The volcanic rocks are about 9.3 Ma old (Duggen et al. 2004). The Alboran Ridge developed due to compressional activity during the Tortonian to the Present (Bourgois et al. 1992).

Drilling during ODP Leg 161 was performed in several regions of the Alboran Sea, revealing that the oldest sediments are derived from Early Miocene rocks and overlie the metamorphic basement. Sedimentation continued until the MSC. An erosional surface represents the MES (Campillo et al. 1992; Maldonado et al. 1992), and deposition was re-established after the MSC.

Evidence for Pleistocene to Holocene deformation was found in seismic sections of the ridge (Comas et al. 1999),

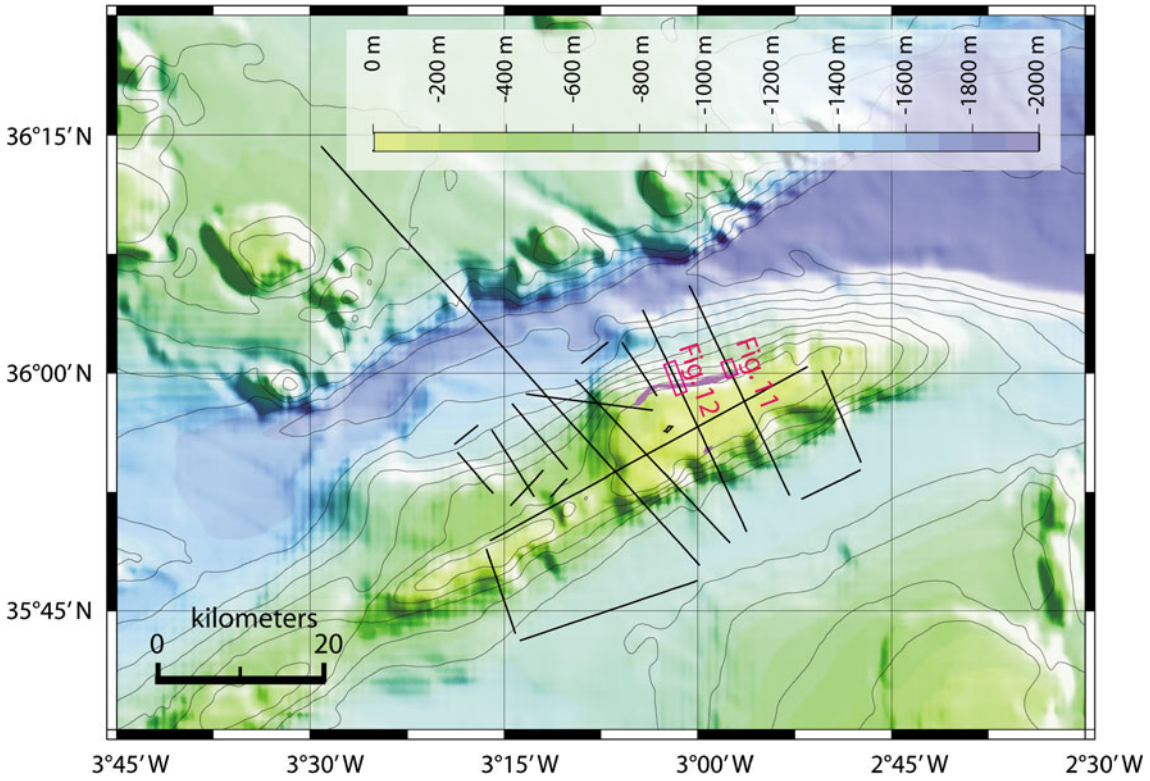

Fig. 5 Bathymetric map (m) of the Alboran Ridge. *Lines* Seismic profiles, *red lines* profiles shown in Figs. 11 and 12; *violet* mapped terraces of the MES

where the MES is characterised by an angular unconformity. Site 976 in the West Alboran Basin reveals two periods of subsidence, one at 11-10.7 Ma (rate of 3 km/10^6 years), another at 2.5-0 Ma (rate of 0.5 km/10^6 years), as well as uplift at 5-2.5 Ma (Comas et al. 1999). Compressional structures have been identified along both the southern and the northern flanks of the ridge. On the southern flank, fault-related uplifting and folding can be found within the Pliocene–Holocene sediments. Comas et al. (1999) proposed that both uplifting due to folding and faulting occurred at different locations along the Alboran Ridge since Late Miocene times. Furthermore, based on a fault population analysis Maestro-González et al. (2008) concluded a reactivation of basement faults at the ridge due to compression during the late Tortonian and Messinian. These authors suggest that the compressional regime probably prevailed also during more recent times.

Materials and methods

Seismic data were acquired using a 600-m-long digital streamer incorporating 144 channels (Mallorca), a 150-m-long 24-channel analog streamer (Bay of Oran and Alboran Ridge), and two GI-guns as seismic sources. The volumes for the generator and injector were 45 and 105 cubic inches respectively, and the pressure within the air chambers was kept constant at 140 bar. The shot distance was 25 m.

For the datasets from the Oran and Alboran study areas, a CMP (common midpoint)-based data processing procedure was used (editing, geometry processing, interactive velocity analysis, stacking, post-stack time migration). The dataset from the Mallorca study area was processed using a CRS (common reflection surface) stacking routine (Mann 2002). The procedure includes stacking over a hyperbolic area and, thus, over neighbouring CMPs. As a result, the fold is increased and, thereby, the data quality (e.g. S/N ratio). The main frequencies were 20–160 Hz for all three study areas. Assigned depths were calculated assuming a seismic velocity of 1,500 m/s for the water column and an average velocity of 1,800 m/s for the post-Messinian sediments.

Seismo-stratigraphic interpretation incorporates previously published information from surrounding areas such as the Valencian Trough (Maillard et al. 2006), the Mallorca and Ibiza channels (Acosta et al. 2003, 2004) and the Alboran Sea (Comas et al. 1999). The correlation was performed on the basis of specific acoustic facies characteristics of individual seismic units and the occurrence of prominent horizons—e.g. the MES.

The locations of seismic profiles acquired during the M69/1 cruise are illustrated in Figs. 3, 4 and 5. Of these, seven are reported in more detail below.

Results

SW shelf of Mallorca

Three seismic profiles from the south-western shelf of Mallorca cover the shelf and upper slope (Figs. 6, 7 and 8). The profile in Fig. 6 has a length of 18 km. In the proximal part, the water depth is about 75 m and the seafloor descends basinwards to a depth of 300 m. The profile in Fig. 7 has a length of about 23 km. On the shallow shelf, the water depth is about 75 m and the seafloor descends south-westwards to 450 m. The profile in Fig. 8 has a length of about 27 km and also strikes perpendicular to the bathymetric contours. In the shallower part of the profile, the water depth is 75–150 m. The seafloor descends to a depth of 375 m towards the SW.

In all seismic profiles for this study area, we identified a prominent high-amplitude reflection with an erosive character in the proximal part of the profiles. This reflection correlates well with the MES of the seismic lines of Acosta et al. (2004). In Fig. 6, the MES is located at 0.55 s TWT in the proximal part, and ascends coastwards to the seafloor, truncating several strong reflections at about 0.5–0.48 s TWT. Adjacent to this truncation, a terrace about 1.5 km wide is present at 0.48 s TWT.

In the distal part of the seismic section in Fig. 7, the MES is downfaulted by 0.05 s TWT. Coastwards of this morphological step, the MES occurs at 0.75 s TWT and ascends at an angle of 1.4° up to a TWT of 0.48 s (approx. 400 m). At this depth, a change in dip is observed, the MES becoming nearly horizontal (0.4°). Coastwards of this 400-m-wide terrace, the MES ascends to 0.34 s TWT (1.5°) before rising more steeply up to 0.19 s TWT. In the proximal part of the profile, the MES has an irregular, near-horizontal morphology.

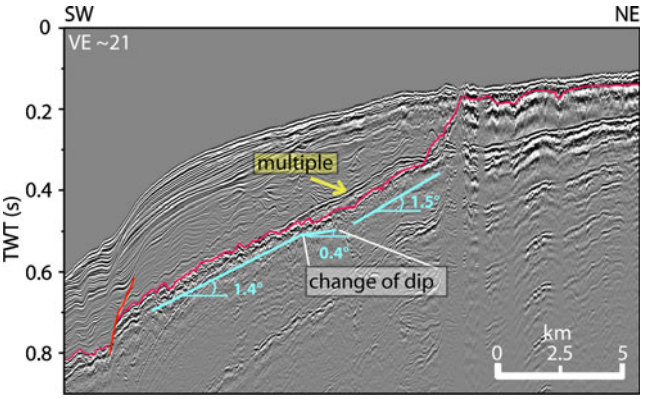

Fig. 7 Seismic section from the SW shelf of Mallorca (for location, see Fig. 3; *VE* vertical exaggeration). In the distal part a fault can be seen, the MES (*red line*) being displaced by about 30 m. The MES ascends up to a TWT of 0.48 s with an angle of 1.4°. At 0.48 s TWT, the MES has a gentle dip of 0.4° for about 1 km. Coastwards, it proceeds more steeply to 0.38 s TWT, where it ascends even more steeply to 0.19 s TWT

In Fig. 8, the MES is observed at about 0.8 s TWT in the distal part and at 0.2 s TWT in the proximal part. At about 0.45 s TWT (approx. 380 m), it forms an approx. 1.5-km-wide terrace and a morphologic step; an incision into the underlying unit can be clearly seen at the foot of this step. This change in morphology occurs at a relatively constant depth interval (380–400 m) in all available seismic data from the Mallorcan shelf, except for one profile. In this profile (not shown), a depression in the MES occurs at 0.45 s TWT, but here the morphology of the underlying unit is generally irregular. The changes in MES morphology on the SW shelf of Mallorca and, in

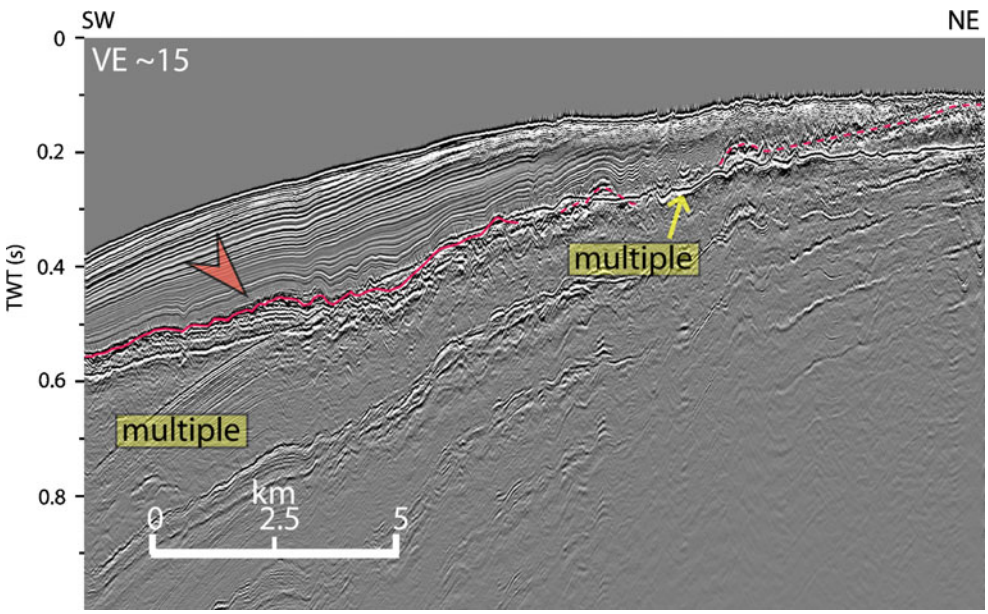

Fig. 6 Seismic section from the SW shelf of Mallorca (for location, see Fig. 3; *VE* vertical exaggeration). The MES (*red line*) truncates internal reflections of the underlying unit at about 0.45 s TWT (*red arrow*), and is overlain by a unit with relatively weak reflections which merges upwards into a unit with strong reflections

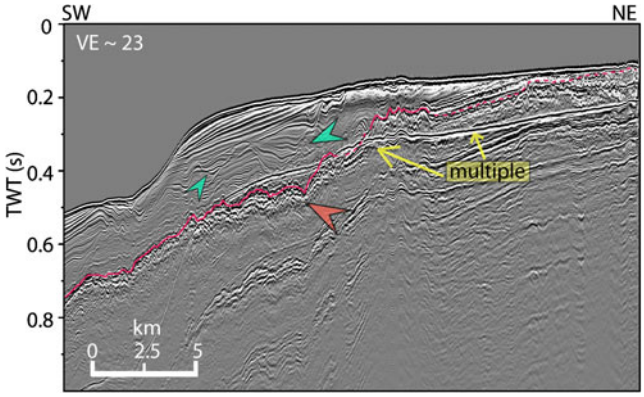

Fig. 8 Seismic section from the SW shelf of Mallorca (for location, see Fig. 3; *VE* vertical exaggeration). At about 0.45 s TWT, the MES (*red line*) is incised into the underlying unit (*red arrow*) and forms a step-like feature about 1.5 km wide. Coastwards, the MES ascends steeply to 0.22 s TWT. Above it, a unit comprising relatively weak reflections is itself truncated at the top. This unconformity is characterized by incisions in the proximal part (*green arrows*), whereas the transition between the two units is more successive in the distal part

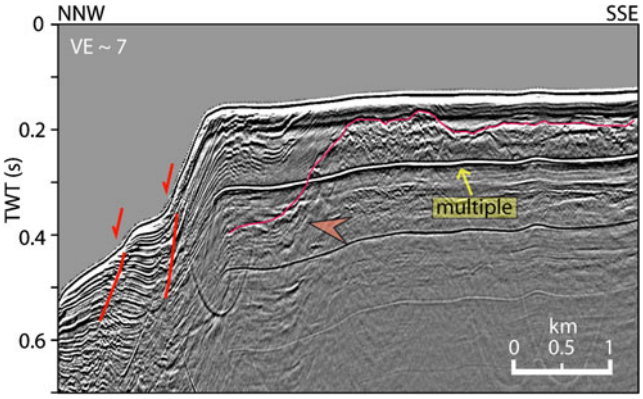

Fig. 10 Seismic section from the Bay of Oran (for location, see Fig. 4; *VE* vertical exaggeration). A strong reflection (*red line*) forms a terrace-like feature at about 0.35 s TWT (*red arrow*), about 500 m wide. Coastwards, the strong reflection ascends to about 0.2 s TWT. In the proximal part of the profile, the reflection is irregular and rugged, probably due to former sub-aerial exposure. Superimposed on the unconformity is a transparent seismic unit which itself is overlain by a unit with basinward-dipping reflections. This latter unit is tilted due to normal faulting in the distal part

particular, the locations of terraces and cliffs are indicated in Fig. 3.

In all seismic profiles, the MES is overlain by two distinct units with different acoustic facies. The lower unit consists of generally continuous, low-amplitude internal reflections parallel or sub-parallel to the MES. In Figs. 6 and 7, undulations in these reflections mirror the irregularities of the MES, and gradually diminish upwards. This lower unit is superimposed by a high-amplitude unit. The transition is marked by an increase in the amplitude of concordant reflections. In Fig. 8, an unconformity marks the boundary between the low-amplitude unit and the overlying unit. In the proximal part of this profile, channels are incised into the low-amplitude unit. The infill deposits of these channels correlate basinwards with higher-amplitude reflections and, accordingly, with the high-amplitude unit of Figs. 6 and 7. Figure 8 also shows a sediment body which overlies the infill deposits of the incised valleys. The internal reflections of the wedge dip basinwards at an angle of about 1°. This unit is notably present only in this seismic profile.

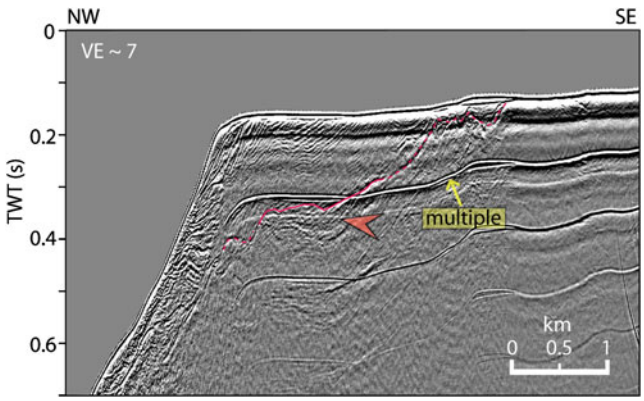

Fig. 9 Seismic section from the Bay of Oran (for location, see Fig. 4; *VE* vertical exaggeration). At about 0.35 s TWT, a morphologic terrace can be seen (*red arrow*) in the prominent reflection (*red line*). This terrace is about 1 km wide; coastwards, the reflection which forms the terrace ascends to 0.18 s TWT. It is overlain by a transparent unit comprising basinward-dipping clinoforms

Bay of Oran

Figures 9 and 10 show seismic sections across the shelf and the adjacent continental slope of the Bay of Oran, at water depths of 75–150 m. The continental slope dips at an angle of about 19°. Both profiles reveal an unconformity below the outer shelf deposits. This unconformity forms a terrace at a TWT of about 0.38 s (320 m). In Fig. 9, the width of this terrace is about 1 km, the corresponding value being about 800 m in Fig. 10. This terrace has been identified on four profiles from this study area (Fig. 4), the unconformity being masked by the seafloor multiple on other profiles.

Coastwards, the unconformity ascends to a TWT of about 0.18 s, where another hummocky terrace approx. 2 km wide is visible (Fig. 10). In this region, a truncation of the underlying deposits at the unconformity can not be clearly identified. Above the deeper terraces occurs a prograding wedge composed of several dipping clinoforms; basinwards, it is tilted due to normal faulting.

Alboran Ridge

Figures 11 and 12 show details of seismic profiles from the northern flank of the Alboran Ridge. In Fig. 11, the seafloor

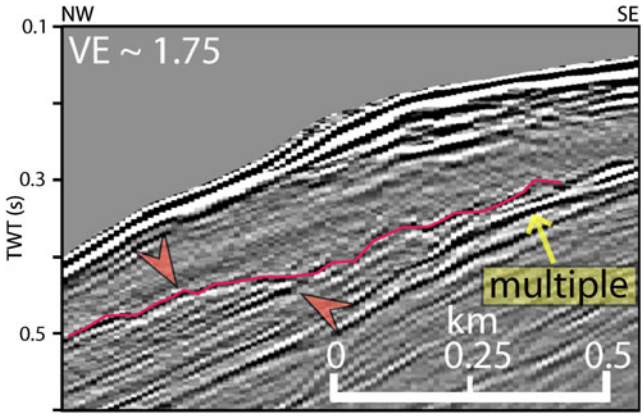

Fig. 11 Seismic section from the Alboran Ridge (for location, see Fig. 5; *VE* vertical exaggeration). At a TWT of about 0.43 s, a reflection (*red line*) truncates the internal reflections of the underlying unit and forms an approx. 150-m-wide, terrace-like feature (*red arrows*). The unconformity is overlain by a transparent seismic unit which, in its proximal part, is characterized by a few strong, basinward-dipping reflections just beyond the seafloor

ascends from 0.4 s (300 m) to 0.15 s TWT (112 m). A distinct unconformity underlies the platform edge at approx. 200 ms TWT below the seafloor. At a TWT of 0.43 s (360 m), underlying reflections are clearly truncated at the unconformity. The unconformity shows a change in dip indicating a 250-m-wide terrace-like feature, above which a transparent seismic unit occurs. Close to the seafloor, some high-amplitude reflections dip basinwards.

In Fig. 12, the seafloor ascends from 0.67 s (502 m) to 0.14 s TWT (105 m). There is a significant change in dip of the seafloor at 0.15 s TWT (112 m), which marks the margin of the flat-topped ridge. At about 0.45 s TWT (approx. 360 m), a 350-m-wide terrace-like feature similar to that in

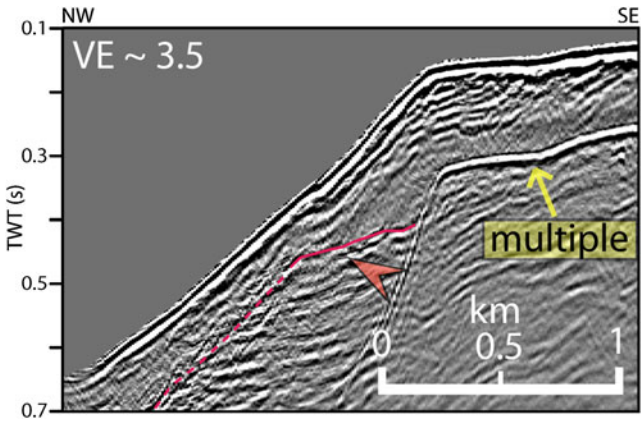

Fig. 12 Seismic section from the Alboran Ridge (for location, see Fig. 5; *VE* vertical exaggeration). An irregular rugged reflection (*red line*) at about 0.43 s TWT represents an erosional unconformity (*red arrow*). As in the case of the Bay of Oran (Fig. 10), this unconformity is overlain by a transparent seismic unit above which basinward-dipping clinoforms are visible

Fig. 10 is present. A transparent seismic unit is again observed to be superimposed on the unconformity. The terrace-like feature was clearly identified on four profiles, mainly along the northern flank of the ridge (Fig. 5).

Discussion and conclusions

Stratigraphy

Mallorca

On the seismic profiles off Mallorca, the morphology of the MES resembles an embayment with cliffs and terraces at its margins but a much smoother morphology at its centre (Fig. 3). This laterally changing MES morphology probably reflects the existence of calmer hydrodynamic conditions in the interior part of the embayment and higher energy along the offshore margins. The transparent unit overlying the MES consists of lower Pliocene sediments, and has been identified in many other parts of the Mediterranean (e.g. Acosta et al. 2004; Maillard et al. 2006). Because of the low reflection amplitudes, it is likely that this unit is composed of hemipelagic sediments which have accumulated during a sea-level highstand. The incisions at the top of this unit can be related to a drop in sea level, presumably dating to the Mid or Late Pliocene. The infill deposits, as well as their distal equivalents, accumulated during the subsequent sea-level rise and highstand. The superimposed sediment body on Fig. 8 with basinward-dipping reflections is interpreted to have formed during Pleistocene to Holocene times.

Bay of Oran

No seismic data from the Bay of Oran have previously been published and the stratigraphy can not be linked to any well data. However, marine and coastal sediments of Neogene age occur in the vicinity of Oran (Cornet et al. 1952). Furthermore, Miocene carbonate platforms are known from onshore sites NW of Oran (Cornée et al. 1994). In the seismic data, a distinct unconformity can be recognized at the base of the progradational unit. There is no indication of sub-aerial exposure within this superimposed unit. We therefore interpret the unconformity as the MES, at which underlying rocks have been eroded during the MSC. The progradational unit is most likely composed mainly of carbonates which were produced on the shelf and exported to the continental slope since the Pliocene. This interpretation is corroborated by the analytical data of Betzler et al. (2010), who found Holocene carbonates unconformably overlying Miocene to Pliocene or older rocks on the outer shelf.

Alboran Ridge

Seismic and sedimentologic data from the Alboran Basin show that the sediments have accumulated on a folded metamorphic basement, while the seismic data from the Alboran Ridge reveal that it is composed of volcaniclastic and volcanic rocks (Hoernle et al. 2003; Duggen et al. 2004). Betzler et al. (2010) show that neritic carbonates are produced on the ridge, which probably was also the case during past episodes of sea-level highstands. Our data suggest that sediments are present on the ridge crest as well as on its flanks. An erosional surface can be seen in the seismic sections which we interpret as the MES. Although the composition of the basement rocks (carbonates or volcaniclastics) is unclear, the pattern of basinward-dipping reflections below the MES suggests the presence of sedimentary strata.

Since terrigenous input from adjacent areas can be neglected, we conclude that the superimposed transparent unit, which partly shows dipping reflections above the MES, consists of material exported from the ridge crest, which is expected to represent an admixture of volcaniclastics and carbonates.

Evolution of erosional terraces

In each of the investigated areas, terrace-like features and morphologic elongated steps coastwards of these are observed along a high-amplitude reflection. Commonly, these may result from normal faulting or submarine landsliding. Assuming faulting, the step would represent the fault plane of the footwall block. If the step is considered to result from mass wasting, it would represent a head scarp upslope of the slide (Locat and Lee 2002). However, a deep-rooted fault should also be observable in the seismic data in the downward prolongation of the escarpment, which is not the case. Furthermore, the spatial extent of a normal fault should be linear. If the escarpment is considered to result from sliding, a curved head scarp should have the concave side facing the basin (Lewis 1971; Dingle 1977). However, these diagnostic features differ from the mapped escarpment and terrace morphology. Off Mallorca, the morphologic step and terraces are present only at the offshore margins of an embayment-like feature, and not in its interior part (Fig. 3). In the Bay of Oran, the step is bended with the convex side facing the deep basin (Fig. 4). At the Alboran Ridge, no distinct step has been observed, which rules out the presence of faulting or sliding. Thus, we conclude that the terraces are formed by erosion and, consequently, the elongated steps represent cliffs which were generated during the MSC.

The presence of terraces at similar depths in three different study areas strongly suggests that a common regional event triggered their development. The notion of a constant sea level in the Western Mediterranean at the depth of the Sicily Sill during the MSC, as proposed by Blanc (2000, 2006) and Meijer and Krijgsman (2005), is consistent with these observations if the terraces evolved contemporaneously and at essentially the same depth.

In the Bay of Oran, the TWT of these terraces corresponds to a depth of approx. 320 m, whereas in the study area on the Alboran Ridge they are found at about 360 m depth. Off Mallorca, the erosional truncation and the terraces of the MES are present at a depth of about 380 m (cf. all values calculated using a velocity of 1,500 m/s for the water column and 1,800 m/s within the sediments). These slight differences in terrace depths could be explained by distinct subsidence and uplift rates in the various study areas. Late Miocene reefs exist about 70 m above present-day sea level in the hinterland of Mallorca (Pomar 1979; Pomar and Ward 1995). According to Haq et al. (1987), sea level was about 70–80 m higher in the Late Miocene than today, but lower values (50–60 m higher sea level) have recently been published (e.g. Müller et al. 2008). Although subsidence during the Pleistocene in the Campos Basin was reported by Pomar and Ward (1995), we conclude that the study area off Mallorca has been relatively stable in terms of vertical movements since the Miocene. The difference between the depths of the Mallorcan and the

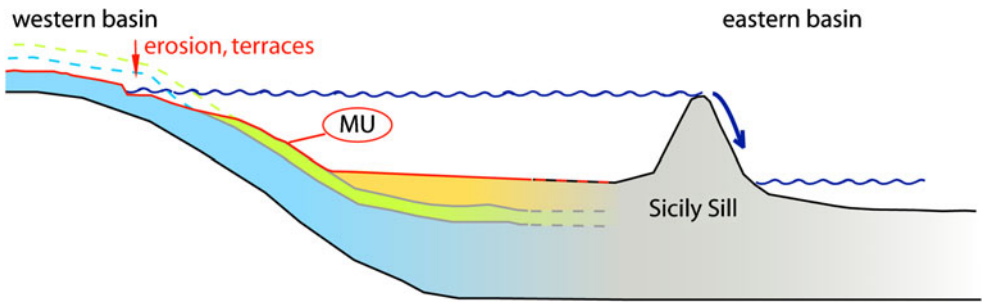

Fig. 13 Schematic sketch illustrating the development of the MES and associated terraces in the Western Mediterranean. During flooding or drawdown events, water overflowed into the eastern basin, while the sea level in the western basin remained constant. These events triggered the development of erosional terraces due to abrasion, dissolution and karstification close to sea level on western Mediterranean continental margins

Alboran Ridge terraces corresponds to an uplift rate of 0.004 mm/year at the ridge, which is consistent with data reported by Comas et al. (1999). In the study area off Oran, the calculated uplift rate based on terrace depth is about 0.012 mm/year in terms of a stable Mallorca scenario. This value is in the order of previously published uplift rates (0.02 mm/year) since the last interglacial (Bouhadad 2001).

As our observations reflect the postulated uplift trends in the Oran (Bouhadad 2001) and Alboran region (Bourgois et al. 1992; Comas et al. 1999; Maestro-González et al. 2008), and a possible minor subsidence trend off Mallorca (Pomar and Ward 1995), we infer a contemporaneous development of the terraces at essentially the same depth in these areas.

Implication of occurrences of erosional terraces

Considering the sea-level history of the Mediterranean basins during the MSC, the Sicily Sill is of central importance. According to our interpretation for the sediment-starved continental slopes investigated in this paper, the margin erosion surface was shaped during periods of sea-level stagnancy when water from the western Mediterranean Sea overflowed into the eastern basin. During these stillstands, hydrodynamic processes and, accordingly, mechanical abrasion resulted in massive erosion of MSC and older deposits. In addition, intensified dissolution and karstification at or close to the sea level could have contributed to the development of the observed terraces and cliffs (Fig. 13).

Since the stratigraphy off Mallorca suggests that no significant uplift or subsidence occurred after the Messinian, we conclude that uplift must have occurred at the Alboran Ridge and the Bay of Oran. Furthermore, we infer that the palaeo-depth of the Sicily Sill corresponds to the observed terrace depth of 380 m off Mallorca, thereby contributing to the ongoing debate about the Sicily Sill depth during the MSC. It remains unclear whether this erosion appeared during the sea-level drawdown (Blanc 2000, 2006), during sea-level fluctuation in the MSC (Gargani and Rigollet 2007) or during the terminal flooding at the end of the MSC (Meijer and Krijgsman 2005). In the case of rapid flooding (Blanc 2000, 2006; Garcia-Castellanos et al. 2009), hydrodynamic processes would not have the potential for massive erosion of the subsurface. Even within such a scenario, however, modelling of the genesis of evaporitic sequences in the Mediterranean suggests that, during an early drawdown of the sea level, water spilled over the Sicily Sill and stagnated in the western basin during some thousand years (Blanc 2000, 2006). Such a protracted period of sea-level stagnancy would plausibly suffice to erode the continental shelves and to produce the detected terraces. Consequently, our observations support all those scenarios which accommodate long-term sea-level stagnancies during the MSC.

Future work should focus on areas of minor sediment input to validate this hypothesis. In such settings, the geometries of the continental slopes are essentially affected only by hydrodynamic processes—e.g. erosion at the wave base or in the breaker zone. Such data could provide valuable information on the sea-level history of the time period in question. Furthermore, if this concept were to be verified at other locations of a wider study region, this would be a valuable tool for reconstructing subsidence and uplift rates along the Western Mediterranean margins since the Messinian Salinity Crisis.

Acknowledgements We gratefully acknowledge the scientific party as well as captain and crew of the research vessel *Meteor* for their support during CARBMED cruise M69/1. Thanks go to P. Meijer, an anonymous reviewer and the journal editors for valuable comments which helped improve the manuscript. We would also like to thank Stefan Dümmong for his support by providing a CRS routine. The STRATEC project was funded by the Deutsche Forschungsgemeinschaft (DFG research grant Hu698/16).

References

Acosta J, Muñoz A, Herranz P, Palomo C, Ballesteros M, Vaquero M, Uchupi E (2001) Geodynamics of the Emile Baudot Escarpment and the Balearic Promontory, western Mediterranean. Mar Petrol Geol 18:349–369

Acosta J, Canals M, López-Martínez J, Muñoz A, Herranz P, Urgeles R, Palomo C, Casamor JL (2003) The Balearic Promontory geomorphology (western Mediterranean): morphostructure and active processes. Geomorphology 49:177–204

Acosta J, Canals M, Carbó A, Muñoz A, Urgeles R, Muñoz-Martín A, Uchupi E (2004) Sea floor morphology and Plio-Quaternary sedimentary cover of the Mallorca Channel, Balearic Islands, western Mediterranean. Mar Geol 206:165–179

Alonso-Zarza AM, Armenteros I, Braga JC (2003) Tertiary. In: Gibbons W, Moreno T (eds) The geology of Spain. Geological Society, London, pp 293–334

Alvaro M, Barnolas A, Cabra P, Comas-Rengifo MJ, Fernández-López SR, Goy A, del Olmo P, del Pozo JR, Simo A, Ureta S (1989) El Jurásico de Mallorca (Islas Baleares). Cuad Geol Ibér 13:67–120

Ayadi A, Ousadou-Ayadi F, Bourouis S, Benhallou H (2002) Seismotectonics and seismic quietness of the Oranie region (Western Algeria): the Mascara earthquake of August 18th 1994, Mw = 5.7, Ms = 6.0. J Seismol 6:13–23

Ballesteros M, Rivera J, Muñoz A, Muñoz-Martín A, Acosta J, Carbó A, Uchupi E (2008) Alboran Basin, southern Spain - Part II: neogene tectonic implications for the orogenic float model. Mar Petrol Geol 25:75–101

Barber PM (1981) Messinian subaerial erosion of the proto-Nile Delta. Mar Geol 44:253–272

Barnolas A, Simó A (1984) Sedimentología. In: Barnolas-Cortinas (ed) Sedimentologia del Jurasico de Mallorca, Excursion Guide. Grupo Español Mesozoico, Palma de Mallorca, pp 73–119

Bertoni C, Cartwright JA (2006) Controls on the basinwide architecture of late Miocene (Messinian) evaporites on the Levant margin (Eastern Mediterranean). Sediment Geol 188(189):93–114

Bertoni C, Cartwright JA (2007) Major erosion at the end of the Messinian Salinity Crisis: evidence from the Levant Basin, Eastern Mediterranean. Basin Res 19:1–18

Betzler C, Braga JC, Martin JM, Sanchez-Almazo IM, Lindhorst S (2006) Closure of a seaway: stratigraphic record and facies (Guadix basin, Southern Spain). Int J Earth Sci 95:903–910

Betzler C, Braga JC, Jaramillo-Vogel D, Römer M, Hübscher C, Schmiedl G, Lindhorst S (2010) Late Pleistocene and Holocene cool-water carbonates of the Western Mediterranean Sea. Sedimentology. doi:10.1111/j.1365-3091.2010.01177.x

Blanc P-L (2000) Of sills and straits: a quantitative assessment of the Messinian Salinity Crisis. Deep Sea Res I Oceanogr Res Pap 47:1429–1460

Blanc PL (2002) The opening of the Plio-Quarternary Gibraltar Strait: assessing the size of a cataclysm. Geodin Acta 15:303–317

Blanc P-L (2006) Improved modelling of the Messinian Salinity Crisis and conceptual implications. Palaeogeogr Palaeoclimatol Palaeoecol 238:349–372

Bouhadad Y (2001) The Murdjadjo, Western Algeria, fault-related fold: implications for seismic hazard. J Seismol 5:541–558

Bourgois J, Mauffret A, Ammar A, Demnati A (1992) Multichannel seismic data imaging of inversion tectonics of the Alboran Ridge (western Mediterranean Sea). Geo-Mar Lett 12(2/3):117–122. doi:10.1007/BF02084921

Bridge C, Calon TJ, Hall J, Aksu AE (2005) Salt tectonics in two convergent-margin basins of the Cyprus arc, Northeastern Mediterranean. Mar Geol 221:223–259

Butler RWH, McClelland E, Jones RE (1999) Calibrating the duration and timing of the Messinian salinity crisis in the Mediterranean: linked tectonoclimatic signals in thrust-top basins of Sicily. J Geol Soc 156:827–835

Campillo AC, Maldonado A, Mauffret A (1992) Stratigraphic and tectonic evolution of the western Alboran Sea: late Miocene to Recent. Geo-Mar Lett 12(2/3):165–172. doi:10.1007/BF02084928

CIESM (2008) The Messinian Salinity Crisis from mega-deposits to microbiology−A consensus report. CIESM, Monaco

Clauzon G, Suc J-P, Gautier F, Berger A, Loutre M-F (1996) Alternate interpretation of the Messinian salinity crisis: controversy resolved? Geology 24:363–366

Cohen A (1993) Halite-clay interplay in the Israeli Messinian. Sediment Geol 86:211–228

Comas MC, Platt JP, Soto JI, Watts AB (1999) The origin and tectonic history of the Alboran Basin: insights from Leg 161 results. In: Zahn R, Comas MC, Klaus A (eds) Proc ODP. Sci Results. Ocean Drilling Program, College Station, pp 555–579

Cornée JJ, Saintmartin JP, Conesa G, Muller J (1994) Geometry, paleoenvironments and relative sea-level (accommodation space) changes in the Messinian Murdjajo carbonate platform (Oran, Western Algeria) - Consequences. Sediment Geol 89:143–158

Cornet A, Dalloni M, Deleau P, Flandrin J, Gautier M, Gourinard Y, Gouskov N, Laffite R (1952) Carte géologique de l'Algérie, Echelle 1/500.000, 2ème edn. Gouvernement Général de l'Algérie, Direction du Commerce, de l'Energie et de l'Industrie, Service de la Carte Géologique, Gaillac-Monrocq, Paris

de Lamotte DF, Saint Bezar BA, Bracène R, Mercier E (2000) The two main steps of the Atlas building and geodynamics of the western Mediterranean. Tectonics 19:740–761

Dewey JF, Helman ML, Knott SD, Turco E, Hutton DHW (1989) Kinematics of the western Mediterranean. Geol Soc Lond Spec Publ 45:265–283

Dingle RV (1977) The anatomy of a large submarine slump on a sheared continental margin (SE Africa). J Geol Soc 134:293–310

Domzig A, Yelles K, Le Roy C, Déverchère J, Bouillin J-P, Bracène R, Mercier de Lépinay B, Le Roy P, Calais E, Kherroubi A, Gaullier V, Savoye B, Pauc H (2006) Searching for the Africa-Eurasia Miocene boundary offshore western Algeria (MARADJA'03 cruise). C R Geosci 338:80–91

Duggen S, Hoernle K, van den Bogaard P, Harris C (2004) Magmatic evolution of the Alboran region: the role of subduction in forming the western Mediterranean and causing the Messinian Salinity Crisis. Earth Planet Sci Lett 218:91–108

Esteban M, Braga JC, Martín JM, Santisteban C (1996) Western Mediterranean reef complexes. In: Franseen EK, Esteban M, Ward WC, Rouchy JM (eds) Models for carbonate stratigraphy from Miocene reef complexes of Mediterranean regions. SEPM, Tulsa, pp 55–72

Faccenna C, Becker TW, Lucente FP, Jolivet L, Rossetti F (2001) History of subduction and back-arc extension in the Central Mediterranean. Geophys J Int 145:809–820

Garcia-Castellanos D, Estrada F, Jiménez-Munt I, Gorini C, Fermàndez M, Vergés J, De Vicente R (2009) Catastrophic flood of the Mediterranean after the Messinian salinity crisis. Nature 462:778–781

Garfunkel Z, Almagor G (1984) Geology and structure of the continental-margin off Northern Israel and the adjacent part of the Levantine Basin. Mar Geol 62:105–131

Gargani J, Rigollet C (2007) Mediterranean Sea level variations during the Messinian salinity crisis. Geophys Res Lett 34: L10405. doi:10.1029/2007GL029885

Gelabert B, Sabat F, Rodriguez-Perea A (2002) A new proposal for the late Cenozoic geodynamic evolution of the western Mediterranean. Terra Nova 14:93–100

Gueguen E, Doglioni C, Fernandez M (1998) On the post-25 Ma geodynamic evolution of the western Mediterranean. Tectonophysics 298:259–269

Hall J, Calon TJ, Aksu AE, Meade SR (2005) Structural evolution of the Latakia Ridge and Cyprus Basin at the front of the Cyprus Arc, Eastern Mediterranean Sea. Mar Geol 221:261–297

Haq BU, Hardenbol J, Vail PR (1987) Chronology of fluctuating sea levels since the Triassic. Science 235:1156–1167

Hoernle K, Duggen S, Geldmacher J, Klügel A, party sbs (eds) (2003) METEOR Cruise No. 51, Leg 1, Vulkosa: Vulkanismus Ostatlantik-Alboran. GEOMAR, Kiel

Hsü KJ, Ryan WBF, Cita MB (1973) Late Miocene desiccation of the Mediterranean. Nature 242:240–244

Hübscher C, Cartwright J, Cypionka H, De Lange GJ, Robertson A, Suc J-P, Urai JL (2007) Global look at salt giants. Eos Trans AGU 88(16):177. doi:10.1029/2007EO160002

Hübscher C, Tahchi E, Klaucke I, Maillard A, Sahling H (2009) Salt tectonics and mud volcanism in the Latakia and Cyprus Basins, eastern Mediterranean. Tectonophysics 470:173–182

Hübscher C, Betzler C, Grevemeyer I (eds) (2010) Sedimentology, rift-processes and neotectonic in the western Mediterranean, Cruise No. 69, August 08 - September 20, 2006. Meteor-Berichte 10-1, Universität Hamburg, Hamburg

Jenkyns HC, Sellwood BW, Pomar L (1990) A field guide to the Island of Mallorca. Geologists' Association, London

Jolivet L, Faccenna C (2000) Mediterranean extension and the Africa-Eurasia collision. Tectonics 19:1095–1106

Lewis KB (1971) Slumping on a continental slope inclined at 1°–4°. Sedimentology 16:97–110

Locat J, Lee HJ (2002) Submarine landslides: advances and challenges. Can Geotech J 39:193–212

Lofi J, Gorini C, Berné S, Clauzon G, Tadeu Dos Reis A, Ryan WBF, Steckler MS (2005) Erosional processes and paleo-environmental changes in the Western Gulf of Lions (SW France) during the Messinian Salinity Crisis. Mar Geol 217:1–30

Lofi J, Déverchère J, Gaullier V, Gillet H, Gorini C, Guennoc P, Loncke L, Maillard A, Sage F, Thinon I (eds) (2010) Atlas of the Messinian seismic markers in the Mediterranean and Black Seas. CCGM, Paris (in press)

Loncke L, Mascle J, Parties FS (2004) Mud volcanoes, gas chimneys, pockmarks and mounds in the Nile deep-sea fan (Eastern Mediterranean): geophysical evidences. Mar Petrol Geol 21:669–689

Loncke L, Gaullier V, Mascle J, Vendeville B, Camera L (2006) The Nile deep-sea fan: an example of interacting sedimentation, salt tectonics, and inherited subsalt paleotopographic features. Mar Petrol Geol 23:297–315

Maestro-González A, Bárcenas P, Vázquez JT, Díaz-del-Río V (2008) The role of basement inheritance faults in the recent fracture system of the inner shelf around Alboran Island, Western Mediterranean. Geo-Mar Lett 28(1):53–64. doi:10.1007/s00367-007-0089-8

Maillard A, Gorini C, Mauffret A, Sage F, Lofi J, Gaullier V (2006) Offshore evidence of polyphase erosion in the Valencia Basin (Northwestern Mediterranean): scenario for the Messinian Salinity Crisis. Sediment Geol 188(189):69–91

Maillard A, Hübscher C, Benkhelil J, Tahchi E (2010) Deformed Messinian markers in the Cyprus Arc: tectonic and/or Messinian Salinity Crisis indicators? Basin Res (in press). doi:10.1111/j.1365-2117.2010.00464.x

Maldonado A, Campillo AC, Mauffret A, Alonso B, Woodside J, Campos J (1992) Alboran Sea late Cenozoic tectonic and stratigraphic evolution. Geo-Mar Lett 12(2/3):179–186. doi:10.1007/BF02084930

Mann J (2002) Extensions and applications of the Common-Reflection-Surface Stack Method. Logos, Berlin

Mart Y, Bengai Y (1982) Some depositional patterns at the continental-margin of the Southeastern Mediterranean Sea. AAPG Bull 66:460–470

Martín JM, Braga JC, Betzler C (2001) The Messinian Guadalhorce corridor: the last northern, Atlantic-Mediterranean gateway. Terra Nova 13:418–424

Meijer PT, Krijgsman W (2005) A quantitative analysis of the desiccation and re-filling of the Mediterranean during the Messinian Salinity Crisis. Earth Planet Sci Lett 240:510–520

Montadert L, Sancho J, Fail JP, Debyser J, Winnock E (1970) De l'âge tertiaire de la série salifère responsable des structures diapiriques en Méditerranée Occidentale (Nord-Est des Baléares). C R Acad Sci 271:812–815

Montigny R, Edel JB, Thuizat R (1981) Oligo-Miocene rotation of Sardinia: K-Ar ages and paleomagnetic data of Tertiary volcanics. Earth Planet Sci Lett 54:261–271

Müller RD, Sdrolias M, Gaina C, Steinberger B, Heine C (2008) Long-term sea-level fluctuations driven by ocean basin dynamics. Science 319:1357–1362

Pomar L (1979) La evolución tectonosedimentaria de las Baleares: análisis crítico. Acta Geol Hisp 14:293–310

Pomar L (2001) Ecological control of sedimentary accommodation: evolution from a carbonate ramp to rimmed shelf, Upper Miocene, Balearic Islands. Palaeogeogr Palaeoclimatol Palaeoecol 175:249–272

Pomar L, Ward WC (1994) Response of a late Miocene Mediterranean reef platform to high-frequency eustasy. Geology 22:131–134

Pomar L, Ward WC (1995) Sea-level changes, carbonate production and platform architecture: the Llucmajor Platform, Mallorca, Spain. In: Haq BU (ed) Sequence stratigraphy and depositional response to eustatic, tectonic and climate forcing. Kluwer, Amsterdam, pp 87–112

Reeder MS, Rothwell G, Stow DAV (2002) The Sicilian gateway: anatomy of the deep-water connection between East and West Mediterranean basins. Geol Soc Lond Mem 22:171–189

Riding R, Braga JC, Martín JM, Sánchez-Almazo IM (1998) Mediterranean Messinian Salinity Crisis: constraints from a coeval marginal basin, Sorbas, southeastern Spain. Mar Geol 146:1–20

Rizzini A, Vezzani F, Cococcetta V, Milad G (1978) Stratigraphy and sedimentation of a Neogene-Quarternary section in the Nile delta area. Mar Geol 27:327–348

Rouchy JM, Caruso A (2006) The Messinian salinity crisis in the Mediterranean basin: a reassessment of the data and an integrated scenario. Sediment Geol 188(189):35–67

Rouchy JM, Saint Martin JP (1992) Late Miocene events in the Mediterranean as recorded by carbonate-evaporite relations. Geology 20:629–632

Ryan WBF (2009) Decoding the Mediterranean salinity crisis. Sedimentology 56:95–136

Ryan WBF, Cita MB (1978) Nature and distribution of Messinian erosional surfaces−indicators of a several-kilometer-deep Mediterranean in the Miocene. Mar Geol 27:193–230

Sage F, Von Gronefeld G, Déverchère J, Gaullier V, Maillard A, Gorini C (2005) Seismic evidence for Messinian detrital deposits at the western Sardinia margin, northwestern Mediterranean. Mar Petrol Geol 22:757–773

Savoye B, Piper DJW (1991) The Messinian event on the margin of the Mediterranean Sea in the Nice area, southern France. Mar Geol 97:279–304

Stampfli GM, Höcker CFW (1989) Messinian palaeorelief from 3-D seismic survey in the Tarraco concession area (Spanish Mediterranean Sea). Geol Mijnb 68:201–210

Vegas R (1992) The Valencia trough and the origin of the western Mediterranean basins. Tectonophysics 203:249–261